Acta Cryst. (1996). D52, 676–686

X-ray Structure of the Cupredoxin Amicyanin, from *Paracoccus denitrificans*, Refined at 1.31 Å Resolution

LOUISE M. CUNANE, ZHI-WEI CHEN, ROSEMARY C. E. DURLEY AND F. SCOTT MATHEWS

Department of Biochemistry and Molecular Biophysics, Washington University School of Medicine, 660 S. Euclid Avenue, St Louis, MO 63110, USA. E-mail: mathews@fsmiris.wustl.edu

(Received 18 August 1995; accepted 22 January 1996)

Abstract

High-resolution X-ray diffraction data to $d_{min} = 1.31$ Å were collected on a Xuong–Hamlin area detector from crystals of the blue-copper protein amicyanin, isolated from *P. denitrificans*. With coordinates from the earlier 2.0 Å structure determination as a starting point, simulated annealing and restrained positional and temperature factor refinements using the program *X-PLOR* resulted in a final *R* factor of 15.5%, based on 21 131 unique reflections in the range 8.0–1.3 Å. Comparison of the 1.31 Å structure with that at 2.0 Å shows the same basic features. However, the high-resolution electron-density maps clearly reveal additional solvent molecules and significant discrete disorder in protein side chains and within the solvent structure. As a consequence of modelling side-chain disorder, several new hydrogen-bonding interactions were identified.

1. Introduction

Amicyanin is a cupredoxin of 11.5 kDa molecular mass located in the periplasm of a number of methylotrophic bacteria. Its principal function is to accept electrons from methylamine dehydrogenase (MADH), a quinoprotein containing the prosthetic group tryptophan tryptophylquinone, and to transfer them to one or more cytochromes (Husain & Davidson, 1985, 1986). Both amicyanin and MADH are induced when these bacteria are grown with methylamine present as the sole carbon source (Husain & Davidson, 1985, 1986; Husain, Davidson & Smith, 1986). In the case of *Paracoccus denitrificans*, two cytochromes are also induced by methylamine, cytochrome c_{551i} and cytochrome c_{553i}, present in addition to the constitutive periplasmic cytochrome c_{550}. Of these, cytochrome c_{551i} is the most efficient electron acceptor *in vitro* (Husain & Davidson, 1986).

The amino-acid sequence of amicyanin is known for three species of bacteria, *P. denitrificans* (van Spanning, Wansell, Reijnders, Oltmann & Stouthamer, 1990), *Thiobacillus versutus* (Van Beeumen, Van Bun, Canters, Lommen & Chothia, 1991) and *Methylobacterium extorquens* AM1 (Ambler & Tobari, 1985). These sequences are homologous, with approximately 55% identity pairwise. The X-ray structures of amicyanin and apoamicyanin from *P. denitrificans* were described at 2.0 and 1.8 Å resolution, respectively, by Durley, Chen, Lim, Mathews & Davidson (1993). The crystal structure of *T. versutus* amicyanin at 2.15 Å resolution also has been presented (Romero *et al.*, 1994), followed by its NMR structure in solution (Kalverda *et al.*, 1994). In addition, the structures of *P. denitrificans* amicyanin in a binary complex with MADH (Chen *et al.*, 1992), and in a ternary complex with MADH and cytochrome c_{551i} (Chen, Durley, Mathews & Davidson, 1994), have been reported.

Table 1. *Crystal data*

Crystal size (mm)	~ 0.3 × 0.3 × 0.4	
Space group	$P2_1$	
Unit-cell dimensions (Å, °)	$a = 28.95$	
	$b = 56.54$	
	$c = 27.55$	
	$\beta = 96.38$	
Maximum resolution (Å)	Crystal 1	1.92
	Crystals 2 and 3	1.31
Total No. of observations	199399	
No. of unique reflections	21131	
Mean $I/\sigma(I)$	16.7	
Data completion to 1.31 Å (%)	99	
R_{merge}* for the 3 data sets (%)	4.99	

* $R_{merge} = \sum_{hkl} \sum_i |I_i - \langle I \rangle| / \sum \langle I \rangle$.

Amicyanin falls into a distinct class of cupredoxins, separate from the plastocyanins and pseudoazurin, to which it bears most similarity. Amicyanin differs from other cupredoxins of known structure in that it has an additional 20 N-terminal residues, which form the first β-strand. In addition, the loop which contains three of the four copper ligands is the shortest of the cupredoxins, with only two residues between each ligand: Cys-X_2-His-X_2-Met. This results in a tighter coordination geometry at the copper site compared with other blue-copper proteins. Amicyanin has the feature shared by all cupredoxins of an NH···S intramolecular hydrogen bond to the cysteine ligand; this together with an intramolecular hydrogen bond from the N-terminal histidine ligand to a glutamate side chain, probably serves to stabilize the copper coordination. The β-sheet structure of amicyanin envelopes several internally-bound solvent molecules which, by means of bridging hydrogen bonds, link some of the β-strands. These internal water molecules

Table 2. *Merging statistics*

Resolution lower limit (Å)	No. of observations	Reflections collected (Friedels combined)					Reflections collected (Friedels separate)		
		n	% Complete	Mean I	Mean $I/\sigma(I)$	R_{merge} (%)	n	% Complete	R_{merge} (%)
2.24	50404	4307	99.7	10830	91	4.0	8363	96.8	3.7
1.78	51851	4258	100.0	2960	69	4.6	8281	97.2	4.2
1.55	37795	4248	100.0	1043	35	7.3	8053	94.8	6.6
1.41	32762	4225	100.0	600	21	10.5	7873	93.2	9.4
1.31	26587	4093	97.2	396	13	13.3	7210	85.6	12.0
Totals	199399	21131	99.4	3210	46	5.0	39780	93.6	4.6

probably contribute to the overall stability of the tertiary structure.

In this paper we present the structure of amicyanin from *P. denitrificans* refined at 1.31 Å resolution. This structure provides atomic coordinates of high precision from which accurate molecular parameters are obtained. In addition, an increased number of solvent molecules have been defined and several side-chain and solvent molecules observed in discretely disordered conformations. This study is the first example of an amicyanin refined to very high resolution, and the accurate structural information thus obtained will serve as a solid foundation for the continued study of amicyanin alone and within the context of its biological electron-transfer partners.

2. Methods

2.1. *Data collection*

Diffraction quality crystals of amicyanin were prepared by macroseeding as described previously by Lim, Mathews, Husain & Davidson (1986): small crystals grown by vapour diffusion in ammonium sulfate, pH 5–6, were used to seed fresh protein solution equilibrated with 3.0 *M* phosphate buffer (sodium monobasic:potassium dibasic = 90:10). The crystals are monoclinic, in space group $P2_1$ and have unit-cell parameters $a = 28.95$, $b = 56.54$, $c = 27.55$ Å and $\beta = 96.38°$; they grow as approximately equidimensional prisms. Three crystals were used for data collection, each approximately 0.3–0.4 mm. in average dimension. Data were collected at room temperature on a Hamlin multiwire area detector (Hamlin, 1985), using graphite-monochromated X-rays ($\lambda = 1.5418$) produced by a Rigaku RU-200 generator operated at 6 kW. For one of the crystals, the resolution range was 33.25–1.92 Å and for the other two crystals it was 3.25–1.31 Å. The data were scaled and merged using software provided with the detector system (Howard, Nielsen & Xuong, 1985). The overall merging R factor was 4.99% for 199 399 observations of 21 131 reflections. The data are 99% complete to 1.31 Å resolution and have an average signal-to-noise ratio $I/\sigma(I) = 16.7$. Data–collection parameters are summarized in Table 1 and a statistical summary of the merging of the three data sets is given in Table 2, including data with Friedel pair reflections combined and separate. A least-squares fit to a Wilson plot (Wilson, 1949), shown in Fig. 1, resulted in an estimate of the overall B as 9.95 Å^2 and scale 2.97.

2.2. *Refinement procedure*

All refinements, map calculations and geometric analyses were carried out with the *X-PLOR* program package, Version 2.1 (Brünger, 1990). Computer modelling was performed on a Silicon Graphics workstation using the program package *TURBO-FRODO* (Roussel & Cambillau, 1991). Coordinates from the structure of *P. denitrificans* amicyanin refined at 2.0 Å resolution were used to initiate the refinement. All solvent molecules in the 2.0 Å model were removed and isotropic B values of protein atoms were reset to 15 Å^2, followed by a round of simulated annealing, to remove bias which may have been present from the earlier model. Data in the resolution range 8.0–1.31 Å were used throughout. After simulated annealing and 120 steps of positional refinement, the R factor was 33.4%; isotropic temperature factors for individual atoms were

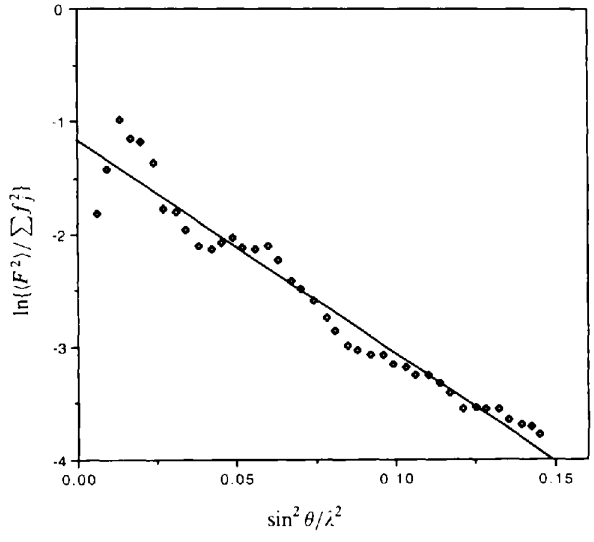

Fig. 1. The Wilson plot for reflections in the range 8.0–1.3 Å resolution, leading to an estimated overall B value of 9.95 Å^2 (Wilson, 1949).

then refined, resulting in a drop to $R = 23.1\%$. The r.m.s. deviations from ideal geometry at this stage were 0.018 Å in bond lengths and 2.94° in bond angles. 80 additional steps of positional refinement gave $R = 22.5\%$, accompanied by a steep decrease in total energy and an improvement in geometry to 0.015 Å and 2.77°.

Electron-density maps were calculated with structure-factor coefficients $2F_o - F_c$ and $F_o - F_c$. Examination of the maps indicated that only minor changes were required in the fitting of the polypeptide chain. As in the 2.0 Å structure, poor density was observed in the loop which includes residues 17–20. After refitting and further positional refinement, water molecules were gradually included in the model; they were selected from peaks greater than 4.0σ in $F_o - F_c$ maps, such that they satisfied the necessary criteria for the formation of at least one hydrogen bond to protein atoms. During the course of successive rounds of remodelling, solvent addition and refinement, both the $2F_o - F_c$ and $F_o - F_c$ maps exhibited significant unaccounted-for density in the vicinity of several surface residues, indicating probable discrete side-chain disorder. At this point, however, alternative side-chain conformers were not modelled into the structure, and care was taken not to misinterpret such electron density as solvent structure.

After 90 water molecules had been added to the model, the R factor was 16.8% and the r.m.s. deviations in bond lengths and angles were 0.012 Å and 2.58°, respectively. It was thought that the structure was then sufficiently well refined and that the data were of sufficiently good quality to justify investigation of the discrete side-chain disorder. An omit map was calculated for each of the 13 residues which appeared to be disordered; this was accomplished by omitting the residue from the model, performing 30 cycles of positional refinement and calculating an $F_o - F_c$ difference map. Several of these residues were subsequently modelled with two alternate side-chain conformers; occupancies were estimated from the relative strengths of the electron density. If, after further refinement and some refitting, the conformers remained in $2F_o - F_c$ density, the $F_o - F_c$ maps were essentially featureless and the temperature factors were sensible, the modelled disorder was retained. In some cases, peaks in $F_o - F_c$ maps which were superimposed on good $2F_o - F_c$ side-chain density were interpretable as incorrectly estimated side-chain occupancies, which were then adjusted accordingly. The inclusion of alternate side-chain conformers caused the R factor to decrease by small increments to $R = 16.4\%$. Water molecules close to these disordered side chains could then safely be added.

More solvent molecules were added after eliminating the requirement for at least one hydrogen bond from water to a protein atom; networks of solvent between symmetry-equivalent amicyanin molecules were being clearly resolved. It became evident in the maps that there were also discretely disordered water molecules present; earlier in the refinement, some of these had appeared as poorly defined peaks in the electron density, which had refined with high temperature factors, and had therefore been rejected. Such density consistently reappeared in the maps, and was fitted as water in mutually exclusive sites, with estimated occupancies, following the guideline that each partial water site must be a potential hydrogen-bond partner to protein or other solvent molecules. Occupancies of water were not refined.

Simulated-annealing (SA) omit maps, with coefficients $2F_o - F_c$, subsequently were calculated to verify the existence of the alternate side chains; these maps provide a view of the selected region unbiased by the rest of the structure (see Hodel, Kim & Brünger, 1992). In addition to confirming the presence of the currently modelled multiple conformers, SA-omit maps were used to clarify other side-chain regions where disorder was suspected, but uncertain. In several such instances, the omit map displayed a widening of density rather than 'split' density, implying either that two discrete conformers lie very close to each other, or that a single conformer is randomly disordered within the unit cell; attempts to model such disorder were not considered justifiable.

An effort was made to identify ambiguous density near the Oγ atom of Ser9, which had been a persistent puzzle throughout the refinement, being too close for assignment as a solvent molecule. This feature had been noted in the 2.0 Å structure, but at the time further investigation was deemed unwarranted. One possibility considered was that Ser9 may have been modified to a phosphoserine, especially in view of the high-molarity phosphate buffer in which the amicyanin crystals had been grown and the large solvent accessibility of this serine residue; on closer examination of the model, however, it appeared that such a bound phosphate would be sterically hindered. An SA-omit map was calculated in order to throw more light on this region; unexpectedly, the map hinted that a methionine residue might be a better fit to the density than serine. Consequently, an anomalous difference Fourier map was calculated in order to locate anomalous scatterers; in addition to the Cu atom, the S atoms in all five methionine residues and the cysteine residue were located as sharp peaks in the map, as shown in Table 3. The highest anomalous peaks were located at Cys92 Sγ and Met98 Sδ, the ligands to copper, reflecting the high degree of order in the copper coordination sphere. However, no anomalous peak was found near the Oγ atom of Ser9, eliminating both a substitution of serine by methionine or modification by phosphate. On checking two independent sequence determinations of amicyanin from *P. denitrificans*, there seems to be no doubt that the residue is, in fact, serine. Earlier in the refinement, Ser9 had been noted as being discretely disordered, including its main-chain atoms, but had been difficult to model as such. The problematic

Table 3. *Anomalous difference peaks*

ρ/r.m.s.(ρ)	
25.0	Cys92 SG
22.4	Met98 SD
18.7	Cu
14.2	Met28 SD
13.5	Met72 SD
11.7	Met71 SD
6.7	Met51 SD

Table 4. *Refinement statistics*

Resolution range (Å)		8.0–1.31
No. of reflections		21098
No. of non-H atoms	Protein	808
	Solvent	123 (+15 with occupancy < 1)
$R = \sum \lvert F_o - F_c \rvert / \sum \lvert F_o \rvert$		0.155
Average temperature factors (Å^2)	All atoms	13.1
	Protein	9.9
	Solvent	30.5
R.m.s. deviations*	Bonds	0.012/0.010
(Å, °)	Angles	2.54/2.52

*R.m.s. deviations from ideal geometry in *X-PLOR* refinement with and without energy restraints on copper-ligand geometry, respectively.

density near Ser9 Oγ may be explained as arising from a partially occupied water, present when serine exists in its second conformer.

The poorly defined loop region (residues 17–20) was also investigated by means of SA-omit maps. During the course of the refinement, the density in this loop had improved only marginally, and it had resisted earlier attempts at remodelling. An SA-omit map clearly indicated an improved fit, requiring a flip of the Asp18–Gly19 peptide bond, thus converting the type III turn into a type II turn; the new fit for this loop refined well. After further refinement, another SA-omit map revealed a possible alternative pathway for the main-chain atoms of residues 17–20, but the density was too weak to fit with any confidence.

The entire refinement of amicyanin employed *X-PLOR* geometric and energetic restraints for the copper site,* as defined previously for the 2.0 Å structure (see Durley *et al.*, 1993). In order to make direct comparisons with copper geometry in other blue-copper proteins, which have been refined with different program packages, the restraints at the copper center were removed and a short positional refinement was carried out.

The final model comprises 808 non-H protein atoms, 123 fully occupied water molecules, nine amino-acid residues with alternate side-chain conformations and 15 discretely disordered water molecules, giving a final $R = 15.5\%$ and r.m.s. deviations from geometric ideality of 0.012 Å and 2.54° for bond lengths and angles, respectively. The removal of the copper-ligand restraints resulted in final $R = 15.5\%$ and r.m.s. deviations from ideality of 0.010 Å and 2.52°. The final refinement statistics are summarized in Table 4.

A Ramachandran plot of the φ–ψ angles (Ramachandran & Sasisekharan, 1968) shows that 94.4% of the non-glycine residues fall within the boundaries of the most favoured regions of the plot and the remaining 5.6% in the additional allowed regions, as defined in the program *PROCHECK* by Laskowski, MacArthur, Moss & Thornton (1993). The maximum average coordinate error was determined from a Luzzati plot (Luzzati, 1952) to be about 0.12 Å, as shown in Fig. 2. Average *B* values for both main-chain and side-chain atoms of each residue are plotted in Fig. 3. It is pleasing to note that the average *B* value for protein atoms (see Table 4) is the same as that estimated from the Wilson plot. Significant peaks in a final difference-Fourier map (above 4σ, maximum 6.9σ) are located in the loop 17–20, at the ambiguous Ser9, near the Cu atom (possibly as a result of anisotropic thermal motion), in the vicinity of two of the disordered residues (Arg99, Lys101) and very close to several solvent molecules whose probable disorder could not

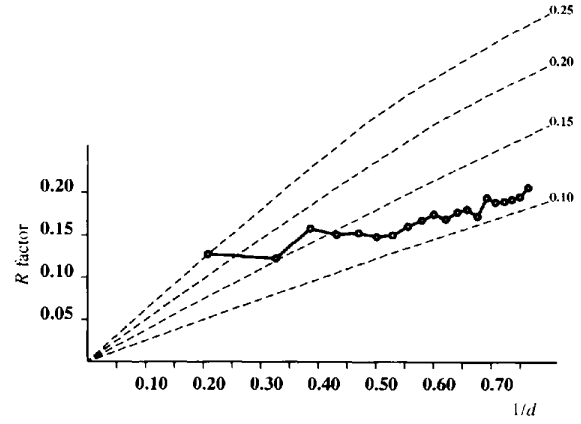

Fig. 2. Luzzati plot of *R* factor *versus* resolution (Å^{-1}) for all observed data in the range 8.0–1.3 Å.

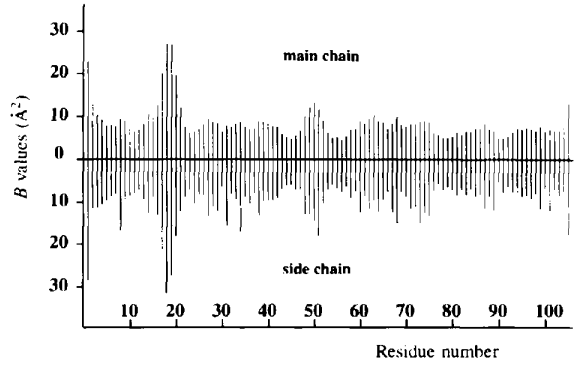

Fig. 3. Average temperature factors (Å^2) for main-chain atoms (above) and side-chain atoms (below) plotted against amino-acid residue number.

* Geometric and energetic parameters restraining the copper site are included in the Protein Data Bank entry (see §3.7).

be modelled; four of the methionine side chains have residual density at their CE atoms, indicating disorder, while the fifth (Met98, the copper ligand) does not.

3. Results and discussion

3.1. *Secondary structure*

The 105 amino-acid chain of amicyanin exhibits a β-sandwich topology, with nine β-strands forming two mixed β-sheets (Fig. 4). This secondary structure is similar to that observed in other classes of cupredoxin, such as the plastocyanins (Guss & Freeman, 1983; Collyer, Guss, Sugimura, Yoshizaki & Freeman, 1990; Redinbo *et al.*, 1993) and pseudoazurin (Petratos, Dauter & Wilson, 1988). The secondary structure of amicyanin, which has been described in detail by Durley *et al.* (1993), is summarized in Fig. 5. Strand 1, containing about 20 amino-terminal residues, and not present in other known cupredoxins, includes an irregular loop which can now be defined more precisely. The loop consists of four residues (6–9); it is located opposite residue 79 on strand 7, with an intervening water molecule which makes four main-chain hydrogen bonds between residues 7 and 79. According to the classification scheme of Chan, Hutchinson, Harris & Thornton (1993), this may best be described as a special β-bulge, type S4, but with the modification of a mediating water molecule in the central hydrogen bond. Notably, the first residue in this bulge is proline, which has been proposed as a possible causative factor in the formation of β-bulges. This β-bulge is conserved in amicyanin from *T. versutus* (Romero *et al.*, 1994), although the sequence is not identical. No clear functional role for the β-bulge is evident; β-strand 1 does not participate in either of the interfacial regions of the MADH–amicyanin–cytochrome crystalline complex, for instance, nor is it directly involved in the configuration of the copper-binding site.

Previously not reported, is the occurrence of two interlocking tight turns, which may be defined as a short piece of 3_{10}-helix, delimited by residues 12 and 16 (Fig. 6); this helical region marks the start of the +3× -crossover connection (as defined by Richardson, 1981) from β-strand 1 to β-strand 2, and is the only helical structure in amicyanin. Plastocyanin (Guss & Freeman, 1983) also contains only one short segment of helical structure, formed by residues 51–56 within the loop joining β-strands 4 and 6, located approximately on the opposite face of the molecule to that in amicyanin.

3.2. *Comparison with the 2.0 Å structure*

There is little overall difference between the amicyanin structure determined at 2.0 Å resolution and that at 1.31 Å resolution. However, the electron-density maps calculated from the high-resolution data provide considerable detail (Fig. 7) and reveal new structural information in the form of multiple side-chain conformers and additional solvent molecules, some of which also have multiple site occupancy.

The r.m.s. difference between the two refined structures is 0.09 for backbone atoms (N, Ca, C, O) and 0.50 for side-chain atoms. The only significant difference in the backbone is in the poorly defined region centered on Gly19, and probably results from differences in the manual modelling of weak electron density. Large side-chain deviations in several cases result from disorder in surface residues, as discussed below; other instances of large side-chain deviations result from the much improved electron-density maps allowing unambiguous fitting of some of the threonine, valine, leucine and isoleucine residues, whose precise rotational orientation was not clear at lower resolution.

Average temperature factors per residue in the 1.31 Å structure have magnitudes comparable to the 2.0 Å structure for the main-chain atoms, but are reduced in many

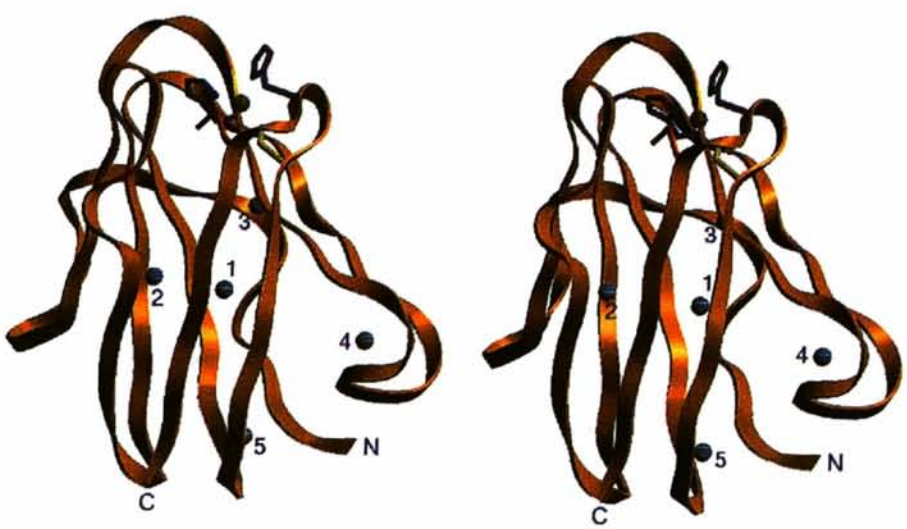

Fig. 4. Ribbon diagram of amicyanin showing its β-sandwich topology and the copper site. Included are the internal waters, numbered 1–5, for waters 201, 202, 204, 207 and 329, respectively. Their interactions with protein main-chain and side-chain atoms are discussed in the text. This diagram was prepared using the molecular graphics program *SETOR* (Evans, 1993).

of the side chains, by as much as 13 Å^2. Their distributions are similar in the two structures, with large B values in both main- and side-chain atoms highlighting the disorder in the 17–20 loop region. As in the 2.0 Å structure, the side chain of Glu8 has a disproportionately large B value; this is probably attributable to multiple occupancy, which has not been modelled in this refinement. Conversely, several side chains have lower B values in the 1.31 Å structure because their discrete disorder has been included in the model; such disorder was not visible in the electron density at 2.0 Å, but was manifest as high temperature factors.

3.3. *The copper site*

In amicyanin, the copper-binding site is formed by a distorted tetrahedral arrangement of ligands coordinated to the metal center, three with short bonds (His53, Cys92 and His95) and one longer one (Met98). Table 5 summarizes the copper–ligand bond lengths and angles obtained from the *X-PLOR* refinements with both the restrained and unrestrained Cu–ligand coordination. Included for comparison are the copper-site geometries of the 2.0 Å amicyanin structure, the *T. versutus* amicyanin at 2.15 Å (Romero *et al.*, 1994; average values from three molecules) and plastocyanin at 1.33 Å resolution (Guss, Bartunik & Freeman, 1992) which was refined using *PROLSQ* (Hendrickson & Konnert, 1980). The geometric parameters from the high-resolution amicyanin structure can be regarded as accurate revisions of those obtained at 2.0 Å resolution.

Because of the lack of estimated standard deviations in coordinates, and hence in the bond lengths and angles, (which could be obtained from a full-matrix, unrestrained refinement), one cannot make substantial claims with respect to small differences in geometry amongst the structures presented in Table 5. It is perhaps permissible, however, to assume that the e.s.d.'s in the copper site are low because of local order imposed by the metal coordination, and that the average coordinate error obtained from the Luzzati plot is an overestimate here. We note that on removing the ligand–copper restraints in the *X-PLOR* refinement, the three short bond lengths to copper become slightly shorter, while the longer Cu—Met98 bond stretches a little; there are no changes in the bond angles around copper after removing restraints. The plastocyanin refinement, with *PROLSQ*, was performed with minimal restraints on the copper geometry. The Cu—His37 and Cu—Cys84 bond lengths are most similar to their counterparts in amicyanin from the unrestrained *X-PLOR* refinement; Cu—His87 and Cu—Met92 differ more markedly from those lengths.

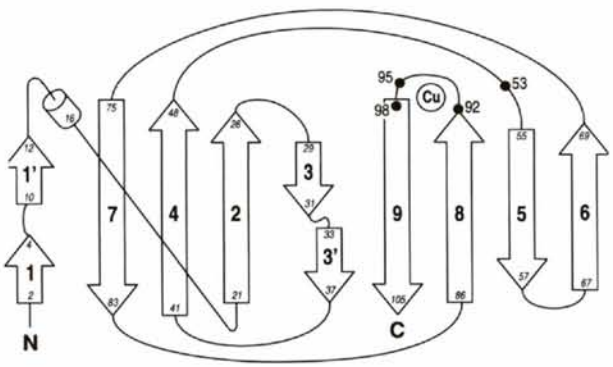

Fig. 5. Topology diagram of amicyanin showing the nine β-strands (represented by arrows) folding into two mixed β-sheets. Strand 1 is interrupted by a β-bulge; a twist in strand 3 allows it to be shared between the two sheets. The crossover connection between strands 1 and 2 contains a short piece of 3_{10}-helix (drawn as a cylinder). Amicyanin contains seven tight turns between consecutive β-strands except between strands 4 and 5, and 7 and 8. The locations of the ligands to copper are indicated by solid circles.

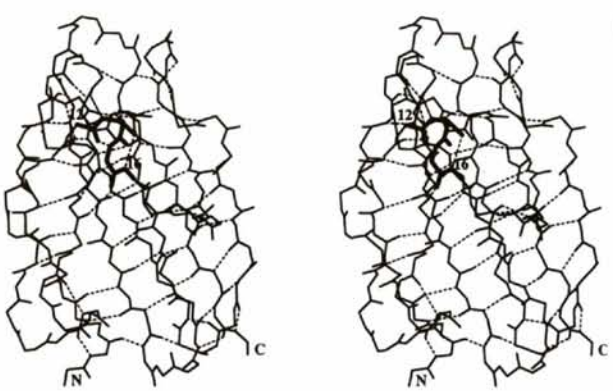

Fig. 6. The main-chain hydrogen-bonding network within the β-sheet structure. The short piece of 3_{10}-helix in the crossover connection between strands 1 and 2 is highlighted (thick lines). This diagram and all subsequent diagrams were produced using the program *TURBO-FRODO* (Roussel & Cambillau, 1991).

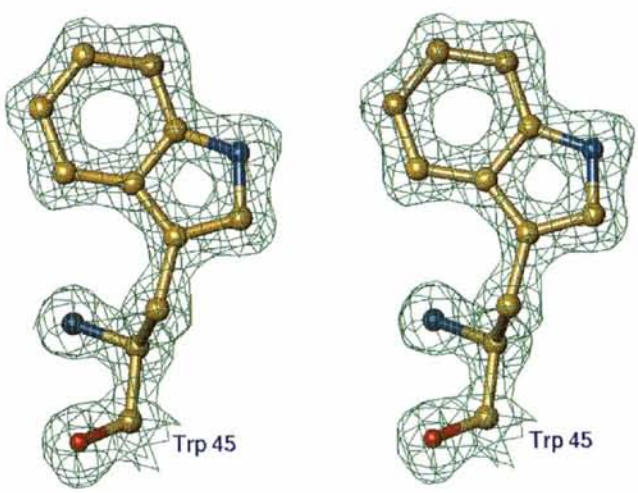

Fig. 7. An example of the quality of electron-density maps obtained from the refinement of amicyanin at 1.3 Å resolution. Residue Trp45 is shown with a $2F_o - F_c$ map calculated using data from 8.0 to 1.3 Å resolution. Contours are at the 1.5σ level.

Table 5. *Copper-binding site geometry*

	Amicyanin 1.31 Å*	Amicyanin 1.31 Å†	Amicyanin 2.0 Å‡	Amicyanin (*T.v.*) 2.15 Å§	Plastocyanin 1.33 Å¶	
Cu—ligand bond lengths (Å)						
Cu—ND1(53)	1.95	1.89	1.95	2.04 (9)	Cu—ND1(37)	1.91
Cu—SG(92)	2.11	2.09	2.15	2.13 (6)	Cu—SG(84)	2.07
Cu—ND1(95)	2.03	1.97	2.00	2.13 (7)	Cu—ND1(87)	2.06
Cu—SD(98)	2.90	2.92	2.89	2.84 (6)	Cu—SD(92)	2.82
Bond angles at Cu (°)						
ND1(53)—Cu—SG(92)	136	136	135	132 (1)	ND1(37)—Cu—SG(84)	132
ND1(53)—Cu—ND1(95)	104	105	109	104 (3)	ND1(37)—Cu—ND1(87)	97
ND1(53)—Cu—SD(98)	84	84	83	84 (2)	ND1(37)—Cu—SD(92)	88
SG(92)—Cu—ND1(95)	112	113	109	111 (2)	SG(84)—Cu—ND1(87)	121
SG(92)—Cu—SD(98)	110	110	109	117 (1)	SG(84)—Cu—SD(92)	110
ND1(95)—Cu—SD(98)	100	100	104	101 (1)	ND1(87)—Cu—SD(92)	101

* This study, *X-PLOR* refinement, copper-ligand restraints applied. † This study, *X-PLOR* refinement, copper-ligand restraints removed. ‡ *X-PLOR* refinement by Durley, Chen, Lim, Mathews & Davidson (1993). § *X-PLOR* refinement of *T. versutus* amicyanin by Romero *et al.* (1994). ¶ *PROLSQ* refinement by Guss, Bartunik & Freeman (1992).

It has been proposed by Han *et al.* (1991), on the basis of resonance Raman spectroscopic measurements, that the cysteine ligand-to-copper conformations in blue-copper proteins are highly conserved in a way that may enhance electron transfer through the Cu–cysteine bond. This is supported by crystallographic evidence from several cupredoxins refined at high resolution, which exhibit near planarity of the Cu–cysteinate moiety. Amicyanin conforms to this pattern, with a Cu—Cys92 Sγ—Cβ—Cα dihedral angle of −176 and Cys92 Sγ—Cβ—Cα—N angle of 179°. The S atom of the methionine ligand is also nearly coplanar with these five atoms, the dihedral angle Met98 Sδ—Cu—Cys92 Sγ—Cβ being −4°.

3.4. *Structural heterogeneity in the protein*

Nine surface residues have been modelled as dual side-chain conformers (Fig. 8): they are Ser9, Lys27, Lys29, Lys38, Lys73, Lys74, Glu75, Arg99 and Lys101. The discretely disordered lysine residues comprise 75% of all lysines in amicyanin. Of interest is that six of the nine observed disordered side chains are located in tight turns. In the type II turn from 73 to 76, three of the four residues are disordered (Fig. 9) and in the type III′ turn from 26 to 29, two are disordered; these turns lack glycine at the second or third position, the presence of which is generally considered favourable for reducing steric hindrance (Richardson, 1981). The main-chain atoms in these two turns sit in well defined density, however, so that the disorder is unlikely to be caused by strain in the polypeptide turns. It is possible that the disorder arises from the presence of four flexible lysine side chains.

In most instances of the disordered external residues, each of the alternate side-chain conformers makes hydrogen bonds to solvent molecules and/or intramolecular or intermolecular hydrogen bonds to protein atoms. This availability of hydrogen-bond partners presumably stabilizes the side chains in discrete conformations, suppressing random orientations. It is interesting to note the correlation of the alternate side-chain occupancies with the side-chain locations which were modelled into the 2.0 Å structure: where one of the conformers has a large occupancy, it is nearly coincident with the 2.0 Å fit, and where two conformers have equal occupancy, the 2.0 Å fit lies either midway between the two, or takes components from each alternate conformation.

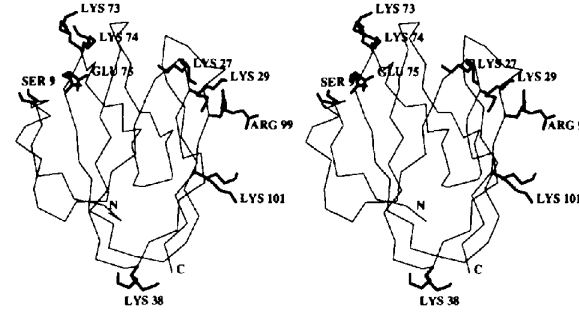

Fig. 8. Cα diagram with the side chains that have been modelled with alternate conformations highlighted in thick lines.

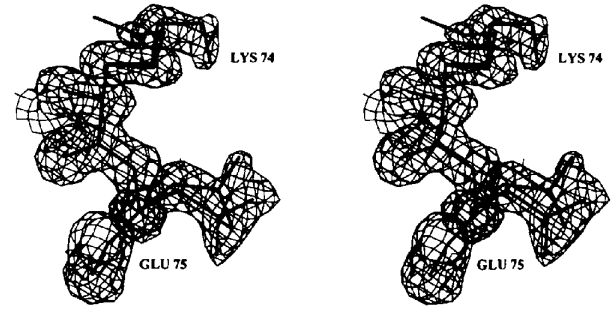

Fig. 9. Side chains Lys74 and Glu75 modelled as dual conformers, in $2F_o - F_c$ density, contoured at the 1.0σ level.

The β-bulge in strand 1 shows evidence of disorder. As discussed earlier, the disorder in Ser9 has been tentatively interpreted as a partially occupied side chain overlapping a partially occupied water molecule. The adjacent Glu8 side chain is also clearly disordered, as indicated by its B value, which is disproportionately large compared with its neighbouring side chains (see Fig. 3). The main-chain atoms of Glu8 and Ser9 also show some evidence of disorder, indicating that there may be more than one conformation of the β-bulge; however, the major bulge conformer does appear to be stabilized by the presence of a water molecule which makes four hydrogen bonds linking strand 1 and strand 7.

The crossover connection between strands 1 and 2 contains the disordered loop of residues 17–20. While residues Ala17 and Ala20 are reasonably well located in the electron density, residues Asp18 and particularly Gly19 are obviously disordered, as demonstrated by their very weak density and high temperature factors (see Fig. 3). It is probable that this loop has multiple conformations within the unit cell.

The ensemble of possible structures obtained from the solution-NMR study of *T. versutus* (*T.v.*) amicyanin was examined in order to compare disorder in solution with that found in the X-ray crystal structures of the *P. denitrificans* (*P.d.*) and *T.v.* amicyanins. In the NMR study, Kalverda *et al.* (1994) found significant structural heterogeneity in the first β-strand, particularly between residues 7 and 11 (6 and 10 in *P.d.* amicyanin), which define the β-bulge. This observation is reflected in the *P.d.* X-ray structure by the disorder seen in Glu8 and Ser9; Romero *et al.* (1994) also note high B values in this part of the *T.v.* amicyanin crystal structure. Surprisingly, the most highly disordered region in the *P.d.* X-ray structure, the 17–20 turn, appears to be well ordered in the *T.v.* NMR structure. In the *T.v.* crystal structure, residue Asp20 (Gly19 in *P.d.*) is also noted as refining with a very high B value, indicating some disorder in this loop.

When comparing disorder in surface regions of proteins in crystal structures, it is useful to consider crystal packing arrangements. *T.v.* amicyanin crystallizes in the trigonal space group $P3_2$, with three independent amicyanin molecules in the asymmetric unit, resulting in different crystal packing from that in *P.d.* amicyanin. Examination of the packing arrangements reveals that in the β-bulge region in *P.d.* amicyanin, Glu8 is exposed to solution, whereas Ser9 makes close contact with a symmetry-related molecule (an intermolecular hydrogen bond, as noted in Table 8); in *T.v.* amicyanin (coordinates from Romero, 1993), the β-bulge in two of the three independent molecules has close contacts with symmetry-related molecules. In this example, the close crystal packing does not appear to prevent disorder, although it is conceivably of smaller magnitude in the crystal structures than it is in solution. In the case of the 17–20 loop, in *P.d.* amicyanin there are no close contacts with symmetry-related molecules. In the *T.v.* amicyanin crystal structure, all three independent molecules have close crystal contacts in this region, except for residue Asp20, which is exposed in two of the three molecules, consistent with their high B values; the third molecule has a more reasonable B value and is in close proximity to a symmetry-related molecule. Thus the disorder in the 17–20 loop, which is marked in *P.d.* amicyanin, appears to be reduced to some extent in *T.v.* amicyanin by crystal packing.

Apart from the crystal packing arrangements in the vicinity of disordered regions, it is possible that other more subtle effects of the crystalline environment are contributing to the disorder. Another factor which is of relevance to the behaviour of macromolecular surface regions is the nature of the solvent. Crystals of both *P.d.* and *T.v.* amicyanin were grown from solutions with 2–3 M salt concentrations, whereas the NMR study was performed in 0.1 M salt solution.

3.5. *Hydrogen bonding in amicyanin*

The structure of amicyanin is composed almost entirely of β-sheet, forming an extensive network of hydrogen bonds among main-chain atoms, in both parallel and antiparallel interactions, as depicted in Fig. 6. The β-ladder is disrupted only by the β-bulge in strand 1 and at the twist in strand 3, where sheet A is terminated and sheet B begins.

There are eight internal neutral polar residues in amicyanin, confirmed by a surface accessibility calculation with a probe molecule radius of 1.6 Å: they are Tyr30, Trp45, Asn47, His53, Asn54, Tyr90, Cys92 and Thr93. All of these side chains participate in intramolecular hydrogen bonds, thereby helping to stabilize the internal structure of amicyanin. Each of the two internal asparagine side chains makes three hydrogen bonds, thus fully satisfying their hydrogen-bonding potential. An uncommon interaction is the hydrogen bond between Trp45(NE1) and Tyr90(OH), where the tyrosine hydroxyl group is acting as an acceptor (see Baker & Hubbard, 1984); Tyr90 OH also acts as a hydrogen-bond donor to an internal water molecule (see *Solvent Structure* below for a discussion of internal water molecules). His53 and Cys92 are two of the four ligands to copper; the hydrogen bonds His53 NE2 to Glu49 OE2 and Asn54 N to Cys92 SG probably contribute to stabilization of the copper coordination sphere. As described by Adman (1991), the existence of at least one NH$\cdots$S hydrogen bond between a main-chain amide N atom and the cysteine ligand, is a feature common to all type I copper proteins that have been structurally characterized.

Each of the 41 external polar or charged side chains in amicyanin is involved in hydrogen-bonding interactions. Of these, 17 take part in intermolecular hydrogen bonds, 24 in intramolecular hydrogen bonds to either main-chain or side-chain atoms, and all but five external polar

Table 6. *Side-chain–main-chain intramolecular hydrogen-bond interactions*

Atom *X*	Atom *Y*	Distance (Å) in 1.31 Å structure	Distance (Å) in 2.0 Å structure*
Ser7 OG	Ser9 O	2.75	(2.77)
Ser9 OG	Pro10 O	2.85	(2.82)
Glu15 OE1	Ala12 N	3.11	3.03
Tyr30 OH	Asn54 O	2.77	2.83
Asp41 OD2	Lys38 N	2.98	2.99
Asn47 OD1	Glu49 N	3.08	(3.06)
Asn47 ND2	Met51 O	2.98	3.03
Asn47 ND2	Met72 O	2.93	3.01
Glu49 OE1	Lys27 N	3.06	3.10
Glu49 OE2	Met28 N	2.93	2.92
Asn54 ND2	Gly69 O	2.98	3.00
Asn54 OD1	Thr93 N	2.82	2.85
Lys74 NZ	Arg48 O	>3.5	3.10
Gln76 OE1	Lys73 N	2.98	3.19
Thr83 OG1	Lys2 O	3.14	3.26
Tyr88 OH	Glu84 O	2.78	2.80
Cys92 SG	Asn54 N	3.64	3.66
Arg99 NE	Pro96 O	2.71	2.73
Arg99 NH2	Pro96 O	3.20	(3.21)

* Distances in parentheses are those which were not noted in the structure refined at 2.0 Å.

Table 7. *Side-chain–side-chain intramolecular hydrogen-bond interactions*

Atom *X*	Atom *Y*	Distance (Å) in 1.31 Å structure	Distance (Å) in 2.0 Å structure
Asp24 OD1	Arg48 NE	2.82	2.86
Asp24 OD1	Arg48 NH2	3.13	3.21
Glu34 OE2	His36 NE2	2.79	(2.92)†
His36 ND1	Glu105 OE1	2.79	3.04
Lys38 NZ	Asp41 OD2	3.23	—
Thr42 OG1	Thr81 OG1	2.74	2.92
Thr44 OG1	Ser79 OG	2.77	2.85
Trp45 NE1	Tyr90 OH	3.05	3.04
Arg48 NH1	Glu75 OE1/OE2*	2.91/3.23	3.16
Glu49 OE2	His53 NE2	2.74	2.71
Asn54 ND2	Thr93 OG1	2.90	2.93
His56 ND1	Thr93 OG1	2.72	2.71
Lys74 NZ	Glu75 OE2	3.34	—
Asp89 OD1	Lys101 NZ*	2.92	(3.34)

* Alternate conformer of disordered side chain. † Distances in parentheses are those which were not noted in the structure refined at 2.0 Å.

side chains are bound by at least one solvent molecule. Tables 6 and 7 summarize intramolecular hydrogen bonds involving the main-chain and side-chain atoms in amicyanin. Included for comparison are the hydrogen-bond distances obtained from the model at 2.0 Å resolution. Both tables contain new information which has come to light with the refinement of the structure at 1.31 Å resolution. Four new intramolecular side-chain to main-chain interactions have been identified; of these, the two consecutive hydrogen bonds Ser7 OG···Ser9 O and Ser9 OG···Pro10 O may be important in helping to stabilize the C-terminal end of the β-bulge in β-strand 1. Additional side-chain to side-chain intramolecular hydrogen bonds derive primarily from the distinguishing of alternate conformers of disordered side chains. Several of these are rather long interactions which may not be strong enough to hold the side chains in well defined orientations. In two instances, the protonation state of histidine can be inferred from its hydrogen-bond partners; His36 is sandwiched between Glu34 and Glu105, both ND1 and NE2 acting as hydrogen-bond donors to the glutamate side chains; NE2 of His53 (a copper ligand) is a hydrogen-bond donor to Glu49 OE2.

Table 8. *Intermolecular hydrogen-bond interactions*

Atom *X*	Atom *Y*	Distance (Å) in 1.31 Å structure	Distance (Å) in 2.0 Å structure
Lys2 NZ	Glu15 OE2	2.82	2.82
Pro6 O	Arg99 NH2	3.00	2.97
Ser9 OG	Ala85 N	3.01	2.99
Glu15 OE1	Glu84 OE2	2.62	2.62
Asp18 OD2/OD1	Lys29 NZ/NZ*	3.06/3.27	3.13
Asp24 OD2	Lys68 NZ	3.08	3.18
Lys27 NZ	Glu105 OE1	3.24	—
Glu31 OE1	Lys68 NZ	2.92	2.90
Lys38 NZ	Glu64 OE2	3.01	—
Asp41 OD2	Glu64 OE1	2.62	2.67
Thr42 OG1	Arg99 NH2*	3.29	—
Gln76 NE2	Thr83 O	2.98	2.99

* Alternate conformer of disordered side chain.

3.6. *Intermolecular interactions*

The number of intermolecular hydrogen-bond interactions found in amicyanin at 2.0 Å has been increased by the addition of several new salt bridges, arising from the alternate conformers found at 1.3 Å. These are included in Table 8. Both O atoms of the carboxylate group of Asp18 now make hydrogen bonds, one to each of the alternate Lys29 side chains. One of the Lys27 conformers makes a weak salt bridge to the C-terminal residue, Glu105. Another newly identified salt bridge is that between Lys38 and Glu64. The existence of the two intermolecular acid interactions noted in the 2.0 Å structure is confirmed in the 1.31 Å structure: Glu15 OE1—Glu84 OE2 and Asp41 OD2—Glu64 OE1 (Fig. 10). These side chains are very clearly defined in electron density, have low B values, and the short bond distances of 2.62 are indicative of strong hydrogen-bond interactions. (*c.f.* The formic acid dimer O—H···O distance of 2.67 Å, Cotton & Wilkinson, 1972.) The local environments of these two interactions are remarkably similar. Glu15 OE2 is also hydrogen bonded to Lys2 NZ, as Glu64 OE2 is to Lys38 NZ; these clusters of charged residues lie isolated in a hydrophobic environment, and the protonation of an acid side chain, necessary for hydrogen-bond formation between acid groups, also allows for local charge balance. In addition to the electrostatic interactions and the hydrogen bonds, there are 14 van der Waals contacts less than 3.5 Å between symmetry-related molecules.

3.7. *Solvent structure*

A total of 138 water molecules have been located in the 1.31 Å amicyanin structure, 123 of which are considered to have full occupancy. 15 water molecules are disordered and have been modelled into multisite locations with estimated occupancies (Fig. 11). The 88 waters which were found in the 2.0 Å structure are also present in the 1.31 Å structure, although several of these are now seen to be discretely disordered. Most of the new solvent molecules which have been revealed at 1.31 Å are located in the hydration shell of the protein; some are grouped into strings of water, linked by hydrogen bonds, the longest consisting of 11 waters; others are collected into polygonal arrangements. Such water networks have been observed in a number of other high-resolution X-ray crystal structures, as reviewed by Frey (1993).

In the 2.0 Å structure, four water molecules were found to be internally bound to the protein. The presence of these internal waters is confirmed in the 1.31 Å structure (Fig. 4), appearing amongst the strongest solvent peaks in the electron-density maps: water 201 anchors the β-bulge on strand 1 to strand 7; 202 makes hydrogen bonds to strands 3, 8 and 9, linking β-sheets *A* and *B*; 204 spans strands 5 and 6; and water 207 makes three hydrogen bonds, stabilizing the turn between residues 58 and 61. Amicyanin from *T. versutus* (Romero *et al.*, 1994), which crystallizes with a trimeric arrangement of amicyanin molecules in the asymmetric unit, contains solvent molecules bound at the same internal sites, in each of the three monomers, with the exception of 207, which appears in only two monomers. It seems likely that these internal water molecules contribute significantly to the integrity of the folded protein. Refinement of the 1.31 Å structure has revealed an additional internal water molecule (329) (Fig. 4), which forms a bridge between the carbonyl O atoms of Lys2, on strand 1, and Glu84, on strand 7, thus helping to stabilize the N-terminal residues. Water 329 has been fitted to weak density, however, and is probably partially occupied, which is not unexpected considering its close proximity to bulk solvent and therefore its increased mobility.

A water molecule of interest is that which is bound to the solvent-exposed copper ligand His95, at the NE2 atom (Fig. 12). It was previously noted by Durley *et al.* (1993) that this solvent molecule, (258 in this model), has analogues in both plastocyanin and azurin. Its involvement in electron transfer in azurin has been suggested (Van de Kamp *et al.*, 1991). In the 1.31 Å amicyanin maps, this water is clearly disordered and has been modelled into two sites, 1.61 Å apart, with occupancies estimated as 0.75 and 0.25, and *B* values of 13 and 22 Å^2. Water 258 also makes a hydrogen bond to Thr87 O of a symmetry-related amicyanin molecule. Of note, is that water 258 is conserved in apoamicyanin (Durley *et al.*, 1993), the binary electron-transfer complex between methylamine dehydrogenase (MADH) and amicyanin (Chen *et al.*, 1992) and the ternary complex between MADH, amicyanin and cytochrome c_{551i} (Chen *et al.*, 1994); in the complexes, it is located within the MADH–amicyanin interface, where it forms hydrogen bonds with His95 NE2 of amicyanin, the carbonyl O atoms of Ser56 and Glu101 of the *L* subunit of MADH and another water molecule. Residue 56 of the MADH *L* subunit is adjacent to Trp57, which is the orthoquinone moiety of the redox cofactor tryptophan tryptophylquinone (TTQ), from which it has been postulated that electron transfer to copper occurs, *via* the mediating His95.*

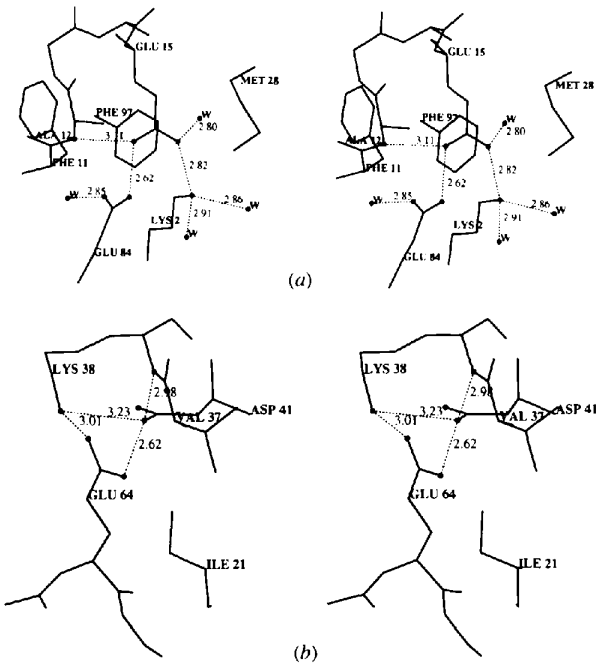

Fig. 10. Interactions between acidic side chains: (*a*) Glu15 and Glu84 (where *W* represents solvent molecules); (*b*) Glu64 and Asp41.

* Atomic coordinates and structure factors have been deposited with the Protein Data Bank, Brookhaven National Laboratory (Reference: 1AAC, R1AACSF). Free copies may be obtained through The Managing Editor, International Union of Crystallography, 5 Abbey Square, Chester CH1 2HU, England (Reference: AM0033).

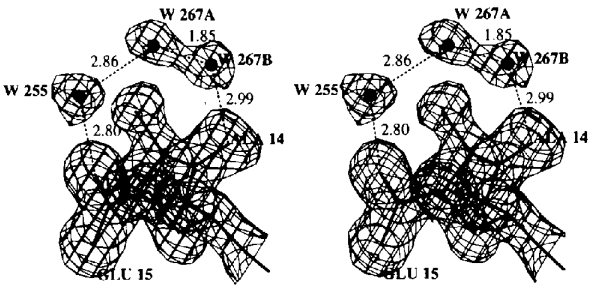

Fig. 11. Example of a discretely disordered water molecule (267*A*, 267*B*) in $2F_o - F_c$ electron density (contoured at 0.85σ). The occupancies of the two sites were estimated as 50:50 and the separation is 1.85 Å.

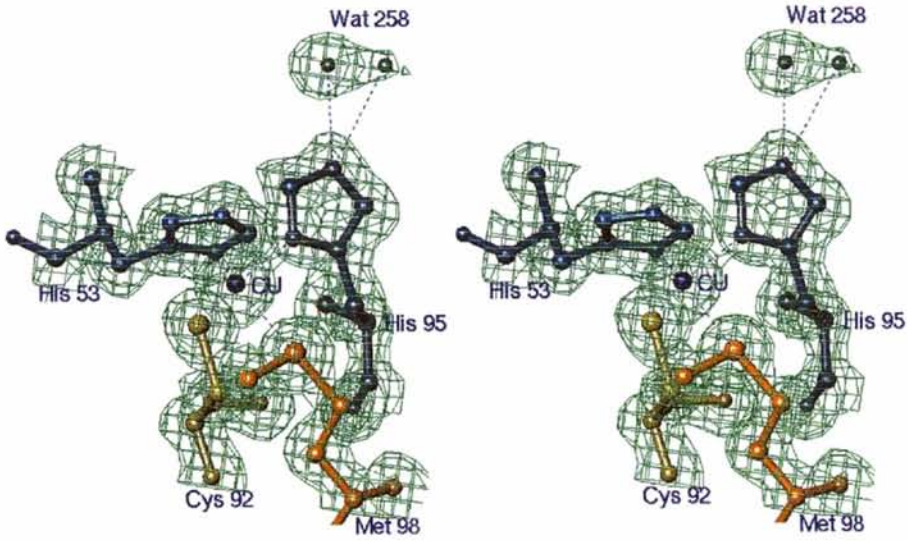

Fig. 12. The copper site in $2F_o - F_c$ electron density (0.8σ level), including the discretely disordered water molecule 258, which may be of importance in electron transfer between methylamine dehydrogenase and amicyanin.

This work was supported by NSF Grant MCB 9419899.

References

Adman, E. T. (1991). *Adv. Protein Chem.* **42**, 145–197.

Ambler, R. P. & Tobari, J. (1985). *Biochem. J.* **232**, 451–457.

Baker, E. N. & Hubbard, R. E. (1984). *Prog. Biophys. Mol. Biol.* **44**, 97–179.

Brünger, A. T. (1990). *X-PLOR. Version 2. 1. A System for Crystallography and NMR*. Yale University, New Haven, Connecticut, USA.

Chan, A. W. E., Hutchinson, E. G., Harris, D. & Thornton, J. M. (1993). *Protein Sci.* **2**, 1574–1590.

Chen, L., Durley, R. C. E., Mathews, F. S. & Davidson, V. L. (1994). *Science*, **264**, 86–90.

Chen, L., Durley, R., Poliks, B. J., Hamada, K., Chen, Z., Mathews, F. S., Davidson, V. L., Satow, Y., Huizinga, E., Vellieux, F. M. D. & Hol, W. G. J. (1992). *Biochemistry*, **31**, 4959–4964.

Collyer, C. A., Guss, J. M., Sugimura, Y., Yoshizaki, F. & Freeman, H. C. (1990). *J. Mol. Biol.* **211**, 617–632.

Cotton, F. A. & Wilkinson, G. W. (1972). *Advanced Inorganic Chemistry*, 3rd ed. New York: Interscience.

Durley, R., Chen, L., Lim, L., Mathews, F. S. & Davidson, V. (1993). *Protein Sci.* **2**, 739–752.

Evans, S. V. (1993). *J. Mol. Graphics*, **11**, 134138.

Frey, M. (1993). *Topics in Molecular and Structural Biology*, edited by E. Westhof, pp. 98–147. Boca Raton: CRC Press.

Guss, J. M., Bartunik, H. D. & Freeman, H. C. (1992). *Acta Cryst.* B**48**, 790–811.

Guss, J. M. & Freeman, H. C. (1983). *J. Mol. Biol.* **169**, 521–563.

Hamlin, R. (1985). *Methods Enzymol.* **114**, 416–452.

Han, J., Adman, E. T., Beppu, T., Codd, R., Freeman, H. C., Huq, L., Loehr, T. M. & Sanders-Loehr, J. (1991). *Biochemistry*, **30**, 10904–10913.

Hendrickson, W. A. & Konnert, J. H. (1980). *Biomolecular Structure, Function, Conformation and Evolution*, Vol. 1, edited by R. Srinivasan, pp. 43–57. Oxford: Pergamon Press.

Hodel, A., Kim, S.-H. & Brünger, A. T. (1992). *Acta Cryst.* A**48**, 851–858.

Howard, A. J., Nielsen, C. & Xuong, N. H. (1985). *Methods Enzymol.* **114**, 452–472.

Husain, M. & Davidson, V. L. (1985). *J. Biol. Chem.* **260**, 14626–14629.

Husain, M. & Davidson, V. L. (1986). *J. Biol. Chem.* **261**, 8577–8580.

Husain, M., Davidson, V. L. & Smith, A. J. (1986). *Biochemistry*, **25**, 2431–2436.

Kalverda, A. P., Wymenga, S. S., Lommen, A., Van de Ven, F. J. M., Hilbers, C. W. & Canters, G. W. (1994). *J. Mol. Biol.* **240**, 358–371.

Laskowski, R. A., MacArthur, M. W., Moss, D. S. & Thornton, J. M. (1993). *J. Appl. Cryst.* **26**, 283–291.

Lim, L. W., Mathews, F. S., Husain, M. & Davidson, V. L. (1986). *J. Mol. Biol.* **189**, 257–258.

Luzzati, V. (1952). *Acta Cryst.* **5**, 802–810.

Petratos, K., Dauter, Z. & Wilson, K. S. (1988). *Acta Cryst.* B**44**, 628–636.

Ramachandran, G. N. & Sasisekharan, V. (1968). *Adv. Protein Chem.* **23**, 283–437.

Redinbo, M. R., Cascio, D., Choukair, M. K., Rice, D., Merchant, S. & Yeates, T. O. (1993). *Biochemistry*, **32**, 10560–10567.

Richardson, J. S. (1981). *Adv. Protein Chem.* **34**, 167–339.

Romero, A. (1993). Personal communication.

Romero, A., Nar, H., Huber, R., Messerschmidt, A., Kalverda, A. P., Canters, G. W., Durley, R. & Mathews, F. S. (1994). *J. Mol. Biol.* **236**, 1196–1211.

Roussel, A. & Cambillau, C. (1991). *TURBO-FRODO, Silicon Graphics Geometry Partners Directory*, edited by Silicon Graphics, p. 86. Mountain View, CA, USA.

Spanning, R. M. J. van, Wansell, C. W., Reijnders, W. N. M., Oltmann, L. F. & Stouthamer, A. H. (1990). *FEBS Lett.* **275**, 217–220.

Van Beeumen, J., Van Bun, S., Canters, G. W., Lommen, A. & Chothia, C. (1991). *J. Biol. Chem.* **266**, 4869–4877.

Van de Kamp, M., Silvestrini, M. C., Brunori, M., Van Beeumen, J., Hali, F. C. & Canters, G. W. (1991). *Eur. J. Biochem.* **194**, 109–118.

Wilson, A. J. C. (1949). *Acta Cryst.* **2**, 318–321.